Received: 23 April 2024 | Revised: 21 August 2024 | Accepted: 26 August 2024

DOI: 10.1002/pro.5171

RESEARCH ARTICLE

THE PROTEIN SOCIETY WILEY

HER4 is a high-affinity dimerization partner for all EGFR/HER/ErbB family proteins

Pradeep Kumar Singh[1] | **Soyeon Kim**[2,3] | **Adam W. Smith**[1]

[1]Department of Chemistry and Biochemistry, Texas Tech University, Lubbock, Texas, USA

[2]Division of Cancer Biology, Department of Medicine, MetroHealth Medical Center, Cleveland, Ohio, USA

[3]Department of Medicine, Case Western Reserve University School of Medicine, Cleveland, Ohio, USA

Correspondence
Adam W. Smith, Department of Chemistry and Biochemistry, Texas Tech University, Lubbock, TX 79409, USA.
Email: aw.smith@ttu.edu

Funding information
National Science Foundation, Grant/Award Number: CHE-1753060; Human Frontiers of Science Program, Grant/Award Number: RGP0059/2019; American Lung Association Lung Cancer Discovery Award, Grant/Award Number: LCD-1035035

Review Editor: Jeanine Amacher

Abstract

Human epidermal growth factor receptors (HER)—also known as EGFR or ErbB receptors—are a subfamily of receptor tyrosine kinases (RTKs) that play crucial roles in cell growth, division, and differentiation. HER4 (ErbB4) is the least studied member of this family, partly because its expression is lower in later stages of development. Recent work has suggested that HER4 can play a role in metastasis by regulating cell migration and invasiveness; however, unlike EGFR and HER2, the precise role that HER4 plays in tumorigenesis is still unresolved. Early work on HER family proteins suggested that there are direct interactions between the four members, but to date, there has been no single study of all four receptors in the same cell line with the same biophysical method. Here, we quantitatively measure the degree of association between HER4 and the other HER family proteins in live cells with a time-resolved fluorescence technique called pulsed interleaved excitation fluorescence cross-correlation spectroscopy (PIE-FCCS). PIE-FCCS is sensitive to the oligomerization state of membrane proteins in live cells, while simultaneously measuring single-cell protein expression levels and diffusion coefficients. Our PIE-FCCS results demonstrate that HER4 interacts directly with all HER family members in the cell plasma membrane. The interaction between HER4 and other HER family members intensified in the presence of a HER4-specific ligand. Our work suggests that HER4 is a preferred dimerization partner for all HER family proteins, even in the absence of ligands.

KEYWORDS

EGFR, fluorescence spectroscopy, HER4, Kinases, membrane proteins, receptor tyrosine

1 | INTRODUCTION

Human epidermal growth factor receptor (HER) family proteins play critical roles in development and homeostasis, but they can also drive severe health issues when mutated or overexpressed (Appert-Collin et al., 2015; Tebbutt et al., 2013). There are four members of the HER family, including EGFR (HER1/ErbB1), HER2 (ErbB2), HER3 (ErbB3), and HER4 (ErbB4). EGFR and HER4 are classic receptors with a ligand-binding extracellular domain and an intracellular catalytic domain, while HER2 has no known ligand and HER3 is kinase-deficient (Citri et al., 2003; Lemmon et al., 2014; Riese et al., 1996; Walker, 1998). Generally, ligand binding to HER proteins leads them to dimerize with themselves or other related family members, which promotes tyrosine phosphorylation (Citri & Yarden, 2006; Endres et al., 2014; Yarden & Sliwkowski, 2001). The kinase activity of HER4 is linked

to MAPK (mitogen-activated protein kinase) and PI3K/AKT (phosphatidylinositol 3-kinase/protein kinase B) pathways as well as other downstream signaling events (Carpenter, 2003; El-Gamal et al., 2021). A wide range of adapters and signaling proteins dock with these phosphorylated tyrosine residues (Carraway & Sweeney, 2001; Hynes & MacDonald, 2009). Unregulated tyrosine kinase activity associated with HER family members may promote tumorigenesis in breast, lung, and colon cancer and several monoclonal antibodies and tyrosine kinase inhibitors (TKIs) that target HERs have been approved by the FDA to treat cancer patients (Fujiwara et al., 2014; Hynes & MacDonald, 2009; Kumagai et al., 2021; Tebbutt et al., 2013).

Among HER family receptors, EGFR and HER2 are arguably the most well-studied because of their strong association with various cancers of the lung, brain, and breast. HER3 is a frequent dimerization partner with HER2, and dual anti-HER2/anti-HER3 therapy has demonstrated efficacy in the treatment of breast cancer (Blumenthal et al., 2013; Diwanji et al., 2021; Phillips et al., 2014). In contrast, HER4 is not as commonly associated with cancer. The HER4 protein was first discovered by Plowman et al. in MDA-MB-453 cells while searching for specific ligands for other membranes of the HER family (Plowman et al., 1993). HER4 protein expression is high in fetal cardiac muscle, brain, and testis, while low in adult tissues, which supports its role in differentiation and development. More recent work has reported its presence in all adult tissues apart from glomeruli and peripheral nerves (Muraoka-Cook et al., 2008; Qiu et al., 2008); however, the expression levels are generally lower than the other HER family members. There are three structural regions in HER family proteins: an extracellular domain (ECD), a transmembrane domain (TMD), and an intracellular domain (ICD) (Sweeney et al., 2000). The HER4 ECD is most similar to HER3, while its cytoplasmic domain exhibits 79% homology with EGFR and 77% with HER2. Despite 60–79% sequence identity, HER proteins differ in many ways beyond their specificity for ligands and effectors. EGFR and HER2 lack phosphorylation sites that allow PI3K subunit p85 interaction; however, HER3 and HER4 contain phosphorylation sites that permit direct PI3K signaling (Yarden & Sliwkowski, 2001). Similarly, EGFR phosphorylation can bind directly to ubiquitin ligase CBL (Casitas B-lineage Lymphoma), while HER4 requires the adaptor protein GRB2 (Growth factor receptor-bound protein 2) for CBL binding (Lucas et al., 2022). As a result of these structural differences, EGFR and HER2 tend to increase cell proliferation, while HER4 generally suppresses cell proliferation (Muraoka-Cook et al., 2008; Xu et al., 2018). Despite this canonical view, many reports have highlighted the potential role of HER4 in cancer development, but the context dependence of HER4's oncogenic role is still not fully understood (Lucas et al., 2022; Roskoski, 2014).

Heterodimerization is an essential step for the activation of catalytically impaired receptor HER3 and the orphan receptor HER2, and many experimental studies of have reported on direct heterodimerization between HER2 and HER3 (Citri et al., 2003; Roskoski, 2014; Tao & Maruyama, 2008; Weitsman et al., 2016). More recently, structural studies have resolved the interactions between HER2 and EGFR (Bai et al., 2023; Diwanji et al., 2021). Functional studies have explored the effects of EGFR or HER2 on HER4 activation (Yarden & Sliwkowski, 2001). For example, kinase-dead HER4 mutants were found to be as efficient as wild-type HER4 in forming a heterodimeric assembly with HER2 (Graus-Porta et al., 1997). Many biophysical techniques have been developed and applied to resolving heterodimers between HER proteins to investigate their role in biology (Brown et al., 2022; Garrett et al., 2003; Nagy et al., 2010; Ogiso et al., 2002; Pryor et al., 2015; Steinkamp et al., 2014; Tao & Maruyama, 2008). High-resolution structure approaches provide atomic level details, but quaternary interactions between membrane proteins need to be resolved in situ because of the chemical complexity of the plasma membrane. Several fluorescence-based methods have been developed to quantify protein interactions in live cells (Martin-Fernandez, 2023; Sankaran & Wohland, 2023; Stoneman & Raicu, 2023). Fluorescence fluctuation spectroscopy (FFS) methods have become valuable for analyzing membrane protein interactions (Bacia et al., 2006; Christie et al., 2020). FFS offers insight into temporal and spatial dimensions that are not easily accessible by super-resolution approaches (Christie et al., 2020). One of these FFS methods is pulsed interleaved excitation fluorescence cross-correlation spectroscopy (PIE-FCCS), which is specialized for a multi-parameter characterization of membrane protein interactions in living cells (Christie et al., 2020; Müller et al., 2005).

Our lab has used PIE-FCCS to investigate conformational coupling across the cell membrane and the multimeric structure of EGFR activated by ligands (Endres Nicholas et al., 2013; Huang et al., 2016). In addition, we have been able to resolve the clinical implications of oncogenic mutants of EGFR using this approach (Brown et al., 2022; Du et al., 2021). The PIE-FCCS technique can be used to determine membrane protein expression

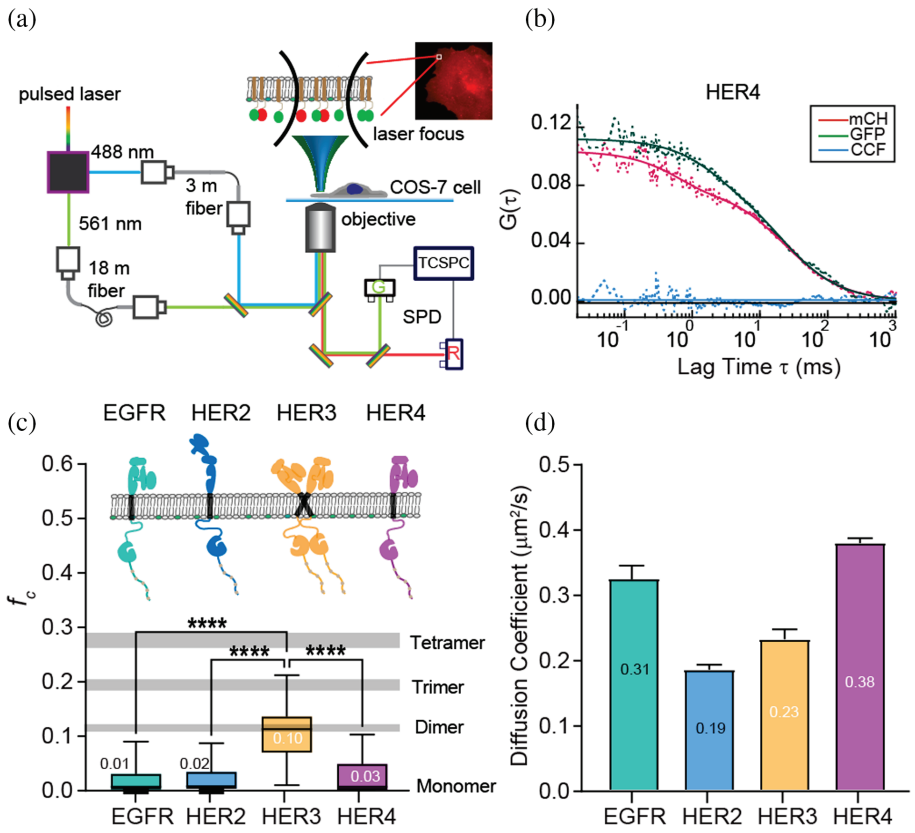

FIGURE 1 (a) Schematic of the PIE-FCCS instrument with two-color, pulsed laser excitation. The inset shows an epifluorescence image of a COS-7 cell expressing HER4-mCherry. A full description of the PIE-FCCS instrument is given in the method section. (b) A representative set of single-cell PIE-FCCS data is shown, with the two autocorrelation functions (ACF) in green and magenta and the cross-correlation function (CCF) in blue. (c) The distribution of f_c values is shown for all of the single-cell measurements of each HER protein without ligand addition. The distributions are represented as boxplots with the median value listed beside each box. The boxes enclose the 25–75 percentile range and the whiskers show the entire range of data. (d) Diffusion coefficients are extracted from the ACF data for each of the measurements shown in panel (d). The data are plotted as the mean of the distribution ± the standard error (SEM).

levels, diffusion coefficients, and the degree of cross-correlation (abbreviated as f_c for fraction of correlation), which is a direct measure of how strongly the proteins interact and diffuse together (Christie et al., 2020). It does not detect immobile aggregates or internalized proteins, as it is primarily sensitive to diffusing proteins. Because f_c depends on co-diffusion, we can interpret the co-diffusing species as stable over the timescale of the transit time ($\sim 10^{-1}$ s), although with PIE-FCCS it is not possible to directly resolve association lifetimes.

In this work, we use PIE-FCCS to evaluate multimerization between HER family proteins and examine the effects of different ligand stimulation conditions. The measurements provide direct evidence for membrane protein interactions in live cells at physiologically comparable expression levels. Overall, we find that HER4 does not self-associate prior to ligand binding; however, it does interact with all other HER family members. The degree of HER4 heterodimerization increases upon stimulation with neuregulin-1 (NRG1, a HER3- and HER4-specific ligand), but is unaffected by EGF (an EGFR-specific ligand) treatment. Heterodimerization between HER4 and all other HER family proteins also increases upon NRG1 stimulation. Our findings suggest that HER4 is a high-affinity heterodimer partner for all of the other HER family proteins.

2 | RESULTS

2.1 | In resting cells, EGFR, HER2, and HER4 are homo-monomers, but HER3 is a homodimer

We first set out to measure the degree of multimerization for each HER family protein. We expressed each protein as two C-terminal fluorescent protein fusion constructs (i.e., HER-mCherry and HER-eGFP) in COS-7 cells and quantified the interactions using PIE-FCCS (Figure 1a). Representative epifluorescence images are shown for COS-7 cells expressing mCherry and eGFP tagged EGFR, HER2, HER3, and HER4 (Figure S1). The optical layout for the PIE-FCCS instrument is outlined in Figure 1a along with a representative COS-7 cell with HER4 protein expression and a schematic of membrane protein diffusion. Figure 1b displays a representative set of single-cell PIE-FCCS data for HER4 proteins. The red and green autocorrelation functions (ACF) are fit to determine the density and mobility of mCherry- and eGFP-tagged HER4 respectively. The blue line shows the cross-correlation function (CCF), the amplitude of which is indicative of correlated diffusion. The fitted values, f_c and diffusion coefficient, for each single-cell measurement are summarized in Figure 1c-d. The distribution of

f_c values for EGFR had a median value of 0.01 (Figure 1c, green). EGFR showed an average diffusion coefficient of 0.31 $\mu m^2/s$ in the resting cell environment (Figure 1d, green). The expression levels of the EGFR protein were calculated to be between 100 and 2000 receptors/μm^2.

Several control constructs were used to interpret the PIE-FCCS results. First, duplex DNA covalently labeled with a red and green dye at the 5′ and 3′ ends (Figure S2, T4-DNA, red) was used as a covalent dimer control mainly for laser alignment. For live cell, membrane protein controls we used two constructs cloned in mammalian expression vectors and transiently transfected into the cells. The first construct is an N-terminal myristoylated peptide (based on the Src protein) with a C-terminal fluorescent protein (eGFP or mCherry), which is monomeric in cells and used as a monomer control. The second construct also contains the same myristoylated peptide but with a leucine zipper motif that drives dimerization, which is used as a dimer control. PIE-FCCS data for these control constructs are shown in Figures S2 and S3. A detailed explanation of the control samples and a numerical model for interpreting the f_c values has been reported in previous work from our group (Kaliszewski et al., 2018).

The PIE-FCCS results for HER2 expressing cells also show near-zero f_c values (median $f_c = 0.02$, Figure 1c, blue), indicating that it does not homodimerize significantly in resting cells. Compared with EGFR, HER2 receptors exhibit a lower diffusion coefficient (0.19 $\mu m^2/s$, Figure 1c, blue). The cross-correlation results are consistent with previous reports that HER2 does not homodimerize in resting cells (Diwanji et al., 2021; Graus-Porta et al., 1997). While surprising, the low diffusion coefficient of HER2 is likely due to interactions with other membrane proteins including HER3 (Jaulin-Bastard et al., 2001; Jeong et al., 2017). We have measured HER2 and HER3 heterodimerization with PIE-FCCS and summarized the results in Figure S10A,B. The median f_c value of 0.18 shows that HER2 and HER3 proteins form a heteromultimer prior to NRG1 ligand binding. This ligand-independent heterodimerization of HER2 and HER3 has been reported in several earlier studies (Diwanji et al., 2021; Pryor et al., 2015; Steinkamp et al., 2014; Weitsman et al., 2016).

PIE-FCCS measurements of HER3 revealed a median $f_c = 0.10$, which indicates significant homodimerization (Figure 1c, yellow). The average diffusion coefficient of HER3 is 0.23 um^2/s (Figure 1d, yellow), which is slower than monomeric EGFR and consistent with ligand-independent dimerization. This result is somewhat surprising as early studies reported that HER3 was incapable of homodimerization (Berger et al., 2004). However, our results are consistent with more recent single-molecule imaging, which provided evidence of HER3 multimerization (Pryor et al., 2015; Steinkamp et al., 2014).

Like EGFR and HER2, HER4 showed near-zero cross-correlation (median $f_c = 0.03$, Figure 1c, magenta), indicating that the proteins are primarily monomeric in COS-7 cells. To the best of our knowledge, no investigation has reported on the dimerization/oligomerization state of HER4 in the absence of ligand stimulation. The diffusion coefficient of HER4 is 0.38 $\mu m^2/s$, (Figure 1d, magenta) which is the highest in comparison to other HER family members, but similar in magnitude to EGFR. Single-cell PIE-FCCS data of all four homomeric interactions (Figure S4) and fit parameters (Table S1) can be found in the supplemental information document. Overall, these PIE-FCCS measurements demonstrate that EGFR, HER2, and HER4 do not self-associate in the absence of ligand, while HER3 exists as a homodimer.

2.2 | HER4 forms a dimer with NRG1 and is unaffected by EGF stimulation

We next tested the effect of ligand stimulation with two common ligands for HER family proteins: EGF and NRG1 (Dawson et al., 2007; Nagy et al., 2010; Plowman et al., 1993). COS-7 cells were transiently transfected with HER4-eGFP and HER4-mCherry and data were collected at cell surface densities between 100 and 1200 molecules/μm^2. We determined the fraction of correlation and diffusion coefficients using the PIE-FCCS data. EGF is not a natural ligand for HER4 and so as expected, EGF stimulation (500 ng/mL) does not change the oligomeric state of HER4 ($f_c = 0.03$), as shown in Figure 2a (blue). The diffusion coefficient of the protein did not change with EGF ligand stimulation, consistent with the f_c values (Figure 2b,c, gray and blue). Upon the addition of NRG1, there was a significant increase in cross-correlation (median $f_c = 0.14$), indicating the formation of a homodimer complex (Figure 2a, magenta; Figure S5C). The HER4 f_c distribution matches the f_c value obtained from a known membrane protein dimer (e.g., GCN4 Figure S2B) and the numerical f_c value (0.07–0.15) expected for dimerization in stochastic model (Kaliszewski et al., 2018). Based on these comparisons we will refer to these complexes as HER4 homodimers. The diffusion coefficient of HER4 after ligand addition, which supports the interpretation of the f_c values (Figure 2b,c, magenta). Single-cell PIE-FCCS data of all four homomeric interactions (Figure S4), and fit parameters (Table S1 & S2) can be found in the supplemental information document.

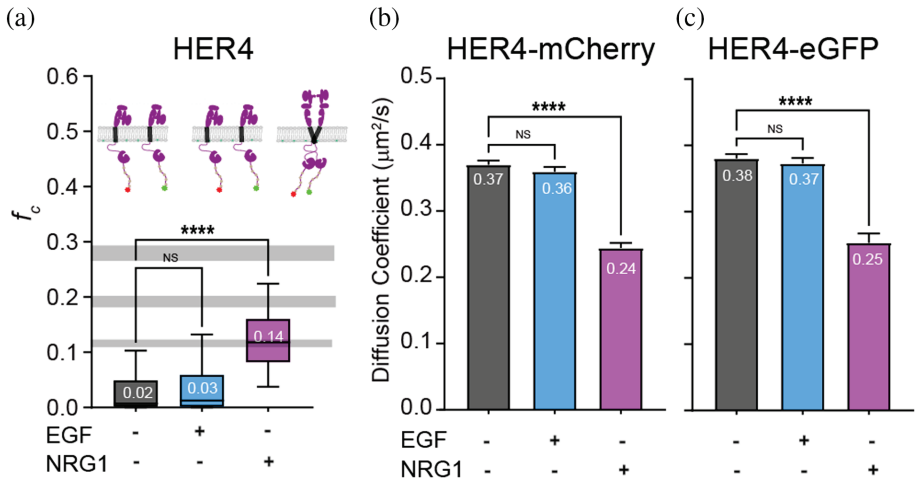

FIGURE 2 Summary of PIE-FCCS measurements of HER4 before and after ligand stimulation. Panel (a) shows the distribution of single-cell f_c values for HER4 homodimerization without ligand stimulation and with EGF or NRG1 addition. An illustration of the HER4 dimerization state is shown above each set of data. The numbers within each box represent the median f_c values. The boxes enclose the 25–75 percentile and the whiskers enclose the entire range of data. Panels (b and c) represent the average diffusion coefficients of each protein before and after ligand treatment. Generally, diffusion coefficients will go down when f_c values go up as larger multimers will diffuse slower than smaller multimers. Diffusion coefficient data is displayed as the mean values ± SEM.

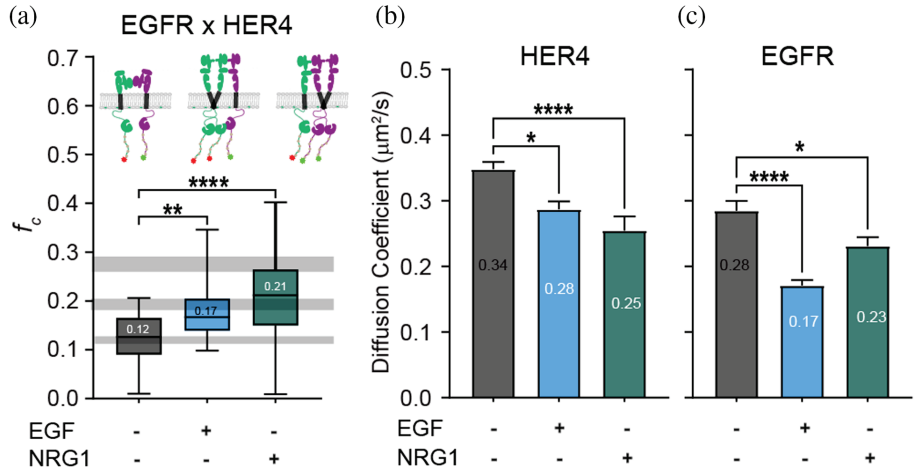

FIGURE 3 PIE-FCCS measurement of HER4-EGFR heteromer with ligands stimulation. Panel (a) shows the degree of cross-correlation (f_c) between HER4 and EGFR proteins before (−) and after (+) EGF or NRG1 stimulation. An illustration of the multimerization states is shown above each set of data. Panels (b and c) represent the average diffusion coefficients of each protein (HER4 and EGFR, respectively) before and after ligands treatment. The numbers within the box represent the samples' median f_c values and average diffusion coefficient. The data are represented as median values with for f_c (A) and mean values with ±SEM for diffusion coefficient (b, c).

2.3 | HER4 and EGFR assemble as a ligand-independent heteromers and undergo increased heteromultimerization with ligand stimulation

To quantify the interactions between HER4 and EGFR, we co-expressed them in live cells and measured the degree of association with PIE-FCCS. Single-cell PIE-FCCS data and fit parameters can be found in Figure S6 and Table S3, and the results are summarized in Figure 3. Interestingly, HER4 and EGFR have a median f_c value of 0.12 without ligand addition, indicating that they heterodimerize significantly in resting cells (Figure 3a, gray). The effect of ligand stimulation on heteromeric interactions was investigated using two ligands (EGF and NRG1). COS-7 cells stably co-expressing HER4-eGFP and EGFR–mCherry were stimulated with 500 ng/mL EGF or 500 ng/mL NRG1 for 15 min and subsequently used for PIE-FCCS measurements. In the presence of EGF, the HER4-EGFR cross-correlation increases

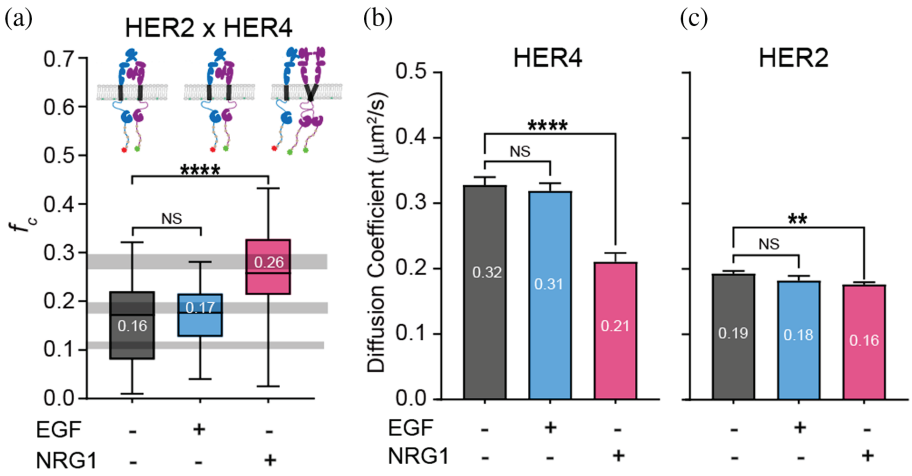

FIGURE 4 PIE-FCCS measurement of HER4 and HER2 upon ligand stimulation. Panel (a) shows the distribution of single-cell f_c values for HER4 and HER2 proteins co-expressed in COS-7 cells before (−) and after (+) EGF /NRG1 ligand treatment. An illustration of the potential interactions based on PIE-FCCS results is also shown in Figure 4a. (b, c) represents the average diffusion coefficients of protein (HER4 and HER2, respectively) before and after ligand treatment. The numbers within the box represent the samples' median f_c values and average diffusion coefficient. All the data are represented as median values for f_c (a) and mean values with ± SEM for average diffusion coefficient (b, c).

slightly ($f_c = 0.17$, Figure 3a, blue), indicating that the ligand promotes heterodimerization, but only to a small degree. Addition of NRG1 ligand nearly doubles the median f_c values from 0.12 to 0.21 (Figure 3a) indicating heteromerization of HER4 and EGFR.

Diffusion coefficients for both receptors support the interpretation of the f_c values (Figure 3a, gray), with reduced mobility observed with EGF and NRG1 treatment compared to in the absence of ligand treatment (Figure 3b,c). EGF ligand treatment slightly reduced the diffusion coefficient of HER4 from 0.34 to 0.28 $\mu m^2/s$ (Figure 3b) while significantly slowing down EGFR from 0.28 to 0.17 $\mu m^2/s$ (Figure 3c). EGF may have induced the formation of multimers within EGFR constructs, explaining the higher reduction in receptor mobility with the treatment (Figure 3c). The NRG1 ligand treatment also significantly reduces the mobility of HER4 proteins (Figure 3b). NRG1 induces homodimerization of HER4 and heteromultimerization between HER4 and EGFR, contributing to the total reduction in protein mobility. The diffusion coefficient of HER4 decreases significantly with NRG1 treatment (Figure 3b $p < 0.0001$) compared to EGF (Figure 3b $p < 0.01$). Like HER4, the mobility of EGFR-mCherry shows the same pattern with EGF treatment compared to NRG1 (Figure 3c $p < 0.0001$). The differences observed in the diffusion and cross-correlation data for the two ligands, EGF and NRG1, suggests that there may be some ligand bias with respect to the size of the hetero-multimers (Huang et al., 2016). This observation could have important functional consequences because larger multimers are correlated with higher levels of tyrosine phosphorylation. The ability of NRG1 to drive larger EGFR/HER4 assemblies could provide a structural mechanism for ligand-bias of downstream effects (Karl et al., 2020).

2.4 | HER4 and HER2 heteromerize in cells prior to ligand binding and assemble into higher order multimers with NRG1 stimulation

Our next step was to examine the heterotypic interactions between HER4 and HER2. HER2 has long been proposed to interact with all other members of the HER family in cell signaling (Graus-Porta et al., 1997). To test this heterotypic interaction, we performed PIE-FCCS measurements by co-expressing HER4-eGFP and HER2-mCherry receptors in COS-7 cells before and after ligand stimulation. Single-cell PIE-FCCS data and fit parameters can be found in the supplemental information document (Figure S7), and the results are summarized in Figure 4. Figure 4a (gray) shows the cross-correlation of HER4 and HER2 in resting cells state with a median f_c value of 0.16. This value supports the interpretation that HER4 interacts directly with HER2 without ligand stimulation. The heteromeric interaction of HER2 with HER4 is significantly higher than the heteromeric interaction of EGFR with HER4 as shown by the median f_c values (Figure S11). Earlier studies have reported ligand-

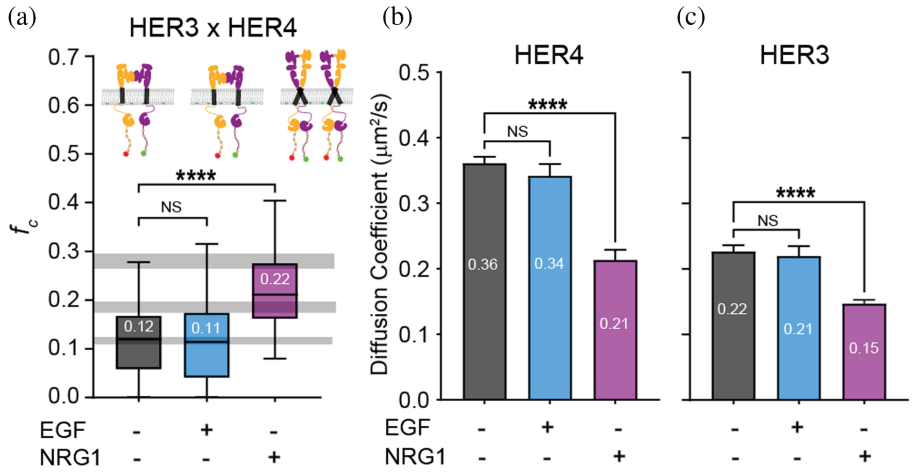

FIGURE 5 Heteromerization of HER4 and HER3 upon EGF and NRG1 stimulation. (a) our PIE-FCCS measurements reveal the heteromultimerization states for HER4 and HER3 in resting cells. The heteromeric interaction is not affected by EGF ligands, but increases with the HER3-/HER4-specific ligand, NRG1. (b, c) The average diffusion coefficients of HER4 and HER3 are shown before and after ligand treatment. The median f_c values and the average diffusion coefficients are displayed inside each box plot. HER,

independent heterodimerization of HER2 and HER3, but to date, there has been no direct experimental investigation of HER4 and HER2 interactions in live cells.

The median f_c value for the complex remained unchanged following EGF stimulation ($f_c = 0.17$, Figure 4a) as well as the diffusion coefficients (Figure 4b,c), which was expected because EGF does not bind HER2 or HER4. However, addition of NRG1 led to an almost two-fold increase of cross-correlation value from 0.16 in resting state to 0.26 after ligand treatment. This increase suggests that NRG1 stimulation drives HER4-HER2 into larger heteromultimers. This is consistent with recent high-resolution structural data that resolved the ligand-bound HER4-HER2 heteromer (Trenker et al., 2023). HER2 proteins exhibit moderate changes in diffusion coefficient after NRG1 treatment compared to HER4, which may be explained by HER4 existing as a mixture of monomers and HER4/HER2 heteromers before NRG1 treatment which then induces HER4 homodimers and larger HER4/HER2 heteromers ($p < 0.01$, Figure 4c). One possible explanation for the slow diffusion of HER2 prior to ligand binding is its extended structure, which could interact with other membrane proteins (Jaulin-Bastard et al., 2001; Jeong et al., 2017). Single-cell PIE-FCCS data and fit parameters can be found in Figure S7 and Table S4.

2.5 | Heteromerization of HER4 and HER3 before and after ligand binding

Next, we measured the degree of interaction between HER4 and HER3 proteins in the absence of ligands and after the addition of EGF and NRG1. The PIE-FCCS experiments were conducted as described above, and single-cell PIE-FCCS data and fit parameters can be found in Figure S8 and Table S5. A median f_c value of 0.12 (Figure 5a, gray) was observed for HER4 and HER3, indicating ligand-independent heteromerization. We next stimulated the receptors with EGF or NRG1 ligands using the same concentrations and incubation conditions as above. Following EGF stimulation, we did not detect any change in the f_c value ($f_c = 0.11$, Figure 5a, blue), which was expected since EGF is not reported to bind HER3 or HER4. The diffusion coefficients of both receptors after EGF treatment also remained unchanged (Figure 5b,c, blue). We next incubated HER4 and HER3 expressing cells with their specific NRG1 ligand. The PIE-FCCS measurements show a larger median f_c value of 0.22 (Figure 5a, magenta), indicating their assembly into larger heteromultimers complex. After NRG1 ligand treatment, the average diffusion coefficient of HER4 and HER3 drastically decreased by 40% (0.35 to 0.21 $\mu m^2/s$) and 32% (0.22 to 0.15 $\mu m^2/s$), respectively, which was further evidence of HER3-HER4 hetero-multimerization (Figure 5b,c).

3 | DISCUSSION

Communication between cells is as vital in an organism as it is in human relationships. Membrane protein receptors, like a listening ear, receive signals and transmit them inside the cell where the decision-making process develops as a complex network of protein–protein interactions (Lemmon & Schlessinger, 2010). Dimerization of RTKs is part of the signal transmission and is therefore integral to cell communication (Lemmon et al., 2014). Understanding how HER proteins are associated with one another is essential for developing more effective therapies and for targeting HER proteins in cancer (Kumagai et al., 2021; Tebbutt et al., 2013). Various

organs in the human body exhibit different levels of HER expression, but this does not always account for the large diversity of behaviors. The phosphorylation and dimerization rates of HER depend on the combination of subtypes in pairs, resulting in diverse kinetic rates (Okada et al., 2022). Homo and heterodimerization of HER family proteins has been shown to correlate with phosphorylation kinetics (Pryor et al., 2015), and recent single-molecule studies have resolved differences in the dimerization stability of EGFR depending on which ligand is present (Freed et al., 2017).

To better understand the molecular assembly of HER receptors in the cell plasma membrane, we investigated the pair-wise interactions of HER proteins in live cells using PIE-FCCS. This approach enabled us to observe the spatiotemporal assembly of HER family proteins in situ and their response to ligand stimulation. We first investigated the homodimerization state of HER proteins without ligand stimulation (Figure 1). From this analysis we conclude that EGFR, HER2, and HER4 are predominantly monomeric, while HER3 forms a ligand-independent homodimer. We then investigated the pair-wise interaction between each of the four HER family proteins. Surprisingly, our PIE-FCCS measurements showed that HER4 forms heteromeric interactions with all other HER family proteins in resting cells. Among the HER4 heteromultimers, HER4-HER2 shows the highest degree of cross-correlation (Figure S11), suggesting it is the highest affinity heterodimer in the absence of ligands consistent with recent cryoEM structures (Trenker et al., 2023). EGF ligand stimulation had little to no effect on the HER4 heterodimers, whereas NRG1 induced higher order heteromultimers.

The existence of ligand-independent multimerization between HER4 and the other EGFR family members could have profound functional implications. Previous studies of ligand-independent homodimerization of EGFR, hypothesized that the dimers are in a dynamic equilibrium between active and inactive states (Arkhipov et al., 2013; Clayton et al., 2005). If this holds true for HER4, then these pre-assembled HER4 heteromultimers could be primed for ligand binding and activation of specific downstream pathways. A recent cryoEM study reports that HER4 heterodimers explore fewer conformations than HER4 homodimers, suggesting they are less structurally dynamic. This could mean that in cells expressing HER4 and other HER family members, the heterodimers could drive specific downstream pathways that would be less likely in the absence of HER4. More functional studies are needed to test these ideas. The expression level of HER4 is typically low in healthy cells, whereas it is considerably overexpressed in some tumor types and in cancer patients that receive EGFR TKIs (El-Gamal et al., 2021; Segers et al., 2020). HER4 overexpression is often associated with poor prognosis, which supports the hypothesis that HER4-EGFR heterodimers may function as oncoproteins in various cancers (Lucas et al., 2022). An analysis of the HER family gene expression profiles in triple-negative breast cancer (defined by the lack of HER2 expression and estrogen and progesterone receptors), showed that increased HER4 expression was linked to a poor prognosis (Kim et al., 2016). The study suggests that HER4 expression could be used as a marker for predicting response to therapy in triple-negative breast cancer (Kim et al., 2016). Crosstalk between EGFR and HER4 modifies the response to HER4 ligands, indicating that signaling by HER4 homodimers differs from that by HER4-EGFR heterodimers. The heterotypic signaling of HER4-EGFR heterodimers has been observed to be associated with oncogenic phenotypes, such as cell proliferation, migration, invasion, and chemoresistance (Haryuni et al., 2019; Tidcombe et al., 2003). The PIE-FCCS measurements reported here provide evidence for heterodimerization between EGFR and HER4 proteins in resting cells, and a significant increase in heteromultimerization after adding the HER4-specific ligand, NRG1. It is worth noting that the EGFR-specific ligand, EGF, had no impact on these heteromeric interactions. Our findings generally agree with previous reports of heterodimerization between HER4 and EGFR.

The prototypical example of RTK heterodimerization is HER2 and HER3, which has been investigated extensively (Diwanji et al., 2021; Graus-Porta et al., 1997; Pryor et al., 2015). HER2 lacks the ability to bind ligands, so its kinase function is only activated when heterodimerized with other members of the HER family (Kiavue et al., 2020). HER3 does not have intrinsic kinase activity (Sierke et al., 1997), and so mainly functions by binding a ligand and then dimerizing with HER2 to activate kinase function (Kol et al., 2014). The role of HER3 homodimerization prior to ligand binding is not fully resolved; however, it may serve as a nucleating interaction for binding other HER proteins as observed in our heterodimerization measurements (Berger et al., 2004; Pryor et al., 2015; Steinkamp et al., 2014; Van Lengerich et al., 2017; Váradi et al., 2019). One study found that a HER3-EGFR chimera forms a heteromer with NRG1 treatment only in the presence of HER2; however, the HER4-EGFR chimera did not require HER2 (Berger et al., 2004). Another study suggests that HER3 is an obligatory heteromeric partner due to its inability to homodimerize (Váradi et al., 2019). The size of the HER3 protein heteromer varies based on whether it is stimulated by EGF or NRG1. A

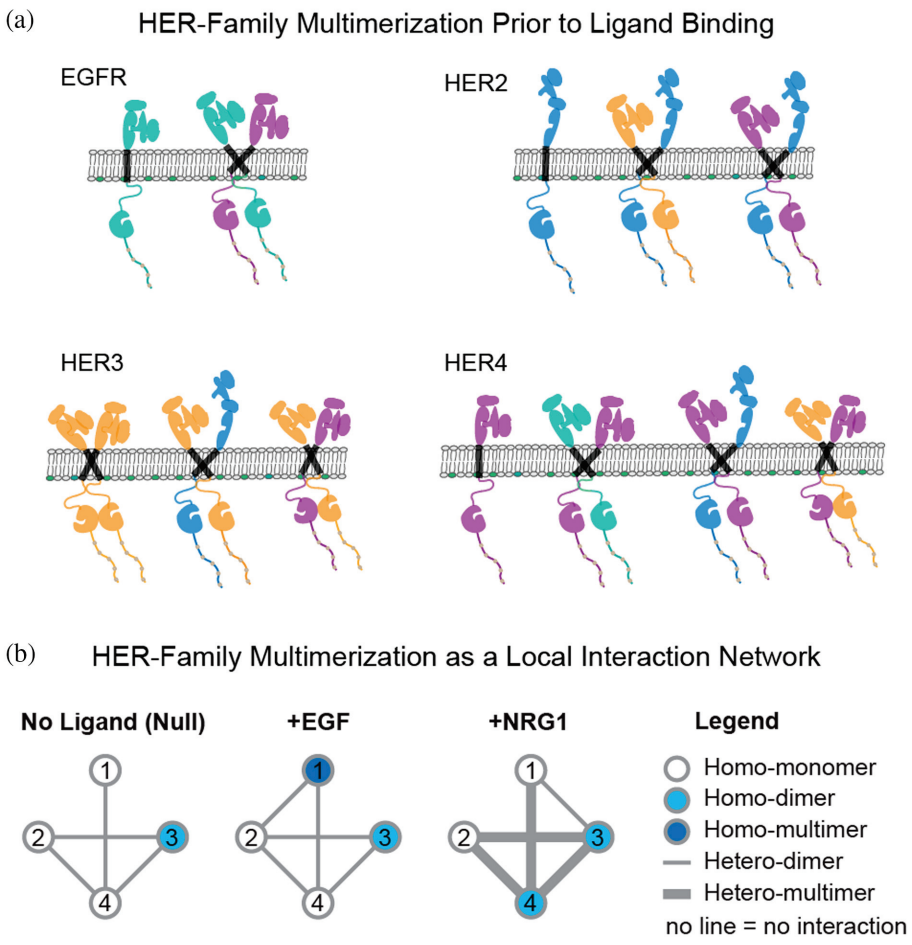

FIGURE 6 Summary of HER family multimerization. (a) Schematic of HER family multimerization without ligands, where only HER3 (yellow) forms ligand-independent homodimers while EGFR (green), HER2 (blue), and HER4 (magenta) are homo-monomers. HER2 and HER3 assemble into ligand-independent heterodimers, while HER4 heterodimerizes with each of the other members: EGFR, HER2, and HER3. (b) The multimerization states can be represented as a local network graph, with each node symbolizing a receptor (colored by homo-multimerization state) and each edge (or line) indicating heterodimerization or heteromultimerization. The *no ligand* (*Null*) graph summarizes the interactions in panel (a). When the system is stimulated with EGF, EGFR assembles into homo-multimers and EGFR-HER2 heterodimers. With NRG1 stimulation, HER4 assembles into homodimers, and heterodimerization increases between all of the receptors except EGFR and HER2. HER, Human epidermal growth factor receptors.

study using single-molecule techniques found that HER3 forms a dimer with EGFR in the presence of NRG, however; it forms higher order oligomers when treated with EGF ligand (Van Lengerich et al., 2017). Another single-molecule study shows that HER2's heteromeric interaction depends on the ligand (Catapano et al., 2023). In the presence of EGFR-specific ligands (EGF and TGF-a), it forms a heteromer with EGFR; however, HER4-specific ligands induce HER2-HER4 heteromer formation, though the process is slow (Catapano et al., 2023). Our PIE-FCCS measurements of HER2-HER3 heteromeric interaction aligned with several previous reports, where we observed substantial heterodimerization in resting cells (Figure S10A).

Based on our PIE-FCCS measurements, we conclude that HER4 is a high-affinity dimerization partner for all HER family proteins. To summarize our findings, we propose the following model outlined in Figure 6. Under basal conditions, HER4 is arranged into heterodimers with all other HER family members in resting cells (Figure 6). These cross-interactions may drive cells to transduce signals and suggests a self-organization principle within these complexes. We have demonstrated that HER signaling can be controlled by ligand binding through the formation of heteromultimers that extend beyond dimers. Our model provides a conceptual framework for future experiments, but additional structural studies are required to elucidate mechanistic details. More work is needed to establish the dimerization interfaces that regulate these interactions and the mechanism by which the heterodimers are activated or inhibited in various liganded states.

4 | MATERIALS AND METHODS

4.1 | Cell culture and preparation for imaging

COS-7 cells were used for this study. COS-7 cells were cultured in Dulbecco's modified Eagle's medium supplemented with 10% fetal bovine serum and 1% penicillin–streptomycin. Transfection of the plasmids was carried out with 70 to 80% confluent cells in 35 mm glass-bottom MatTek dishes. Plasmids coding EGFR, HER2, HER3, and HER4 were subcloned to eGFP-N1 and mCherry-N1 vectors by XhoI and AgeI digestion. The cells were transiently transfected approximately 20 hours before the

data collection with the protein of interest using Lipofectamine 2000 reagent (Thermo Fisher Scientific). A total of 2.5 μg DNA with a 1:1 ratio of mCherry and eGFP-tagged plasmids was used to express both species of fluorescent tagged receptors evenly at a local density of 100–1200 receptors/μm^2 in the cell measurements reported here (Figure S9). During the data collection process, 15–20 cells were selected from each 35 mm dish for PIE-FCCS data collection. The experiments were repeated four to five times on different days, giving a total of 75–100 single-cell measurements per distribution. Before the PIE-FCCS measurements were performed, the media was changed to Opti-MEM I Reduced Serum Medium without phenol red (Thermo Fisher Scientific). For each complex, measurements were taken for both the ligand-free and ligand-stimulated state, using either recombinant human EGF (Sigma-Aldrich, St. Louis, MO) or NRG1 as ligand. In order to stimulate receptor-expressing cells, a stock solution (20 μg/mL) was diluted to 500 ng/mL in Opti-medium (imaging media) and added approximately 15 mins prior to data collection. Data was collected for a maximum of 1 h following stimulation.

4.2 | Control samples

We employed three samples for the alignment of the laser and microscope before data collection. Both 488 and 561 lasers have optical volume differences; therefore, we utilized double-labeled DNA strands to calibrate the volume correction fluorescence value of a sample (Kaliszewski et al., 2018). We applied two samples for the calculation of f_c value of membrane proteins. These negative and positive constructs have a short, lipidated peptide sequence for membrane anchoring and, in the case of GCN4, an α-helical leucine zipper motif for dimerization. From the correlation functions, we obtained f_c and the effective diffusion coefficients of the eGFP and mCH-labeled proteins as described previously. The f_c values are indicative of the co-diffusion of the two receptors (Figure S2A). The median f_c value of 0.01 for SRC (Figure S2B, green) and 0.15 for GCN4 (Figure S2B, blue) are indicative of their monomeric and dimeric state on the plasma membrane. The dimer f_c value of 0.15 is smaller than that observed for a covalent dimer (e.g., duplex DNA, Figure S2B, red). Our duplex DNA control a 40-nucleotide sequence with <50% G-C content [ACA AGC TGG AGT ACA ACT ACA ACA GCC ACA ACG TCT ATA T] was labeled with carboxy-tetramethylrhodamine (TAMRA) at the 5′ end and 6-carboxyfluorescein (FAM) at the 3′ end (Integrated DNA Technologies). An excess of the unlabeled strand was used to anneal the synthesized complementary strand pair as per the supplier's protocols. The double-stranded DNA, labeled with both TAMRA and FAM (TAMRA-40-FAM), was diluted to a final concentration of 100 nM using 10 mM TE buffer. For the 3D sample data collection, laser powers were set to 7 and 7 μW for the 488 nm and 561 nm lasers, respectively.

4.3 | Data collection and analysis

The time–time autocorrelation function is employed for single-color FCS to analyze intensity fluctuations. The results were plotted on a semi-log axis to better view the time scale. In principle, ACF amplitude is inversely proportional to the average number of molecules in the observation area. In FCCS, two fluorescent probes are used to analyze the emission independently of one another using two separate spectrally distinct probes. As a result, both populations have a corresponding ACF, and molecular density can be determined independently. With PIE-FCCS, two laser pulses are phase-delayed calculating the exact arrival time of each laser pulse's emission photons.

The FCCS data were recorded using pulsed interleaved excitation and time-correlated single-photon detection with a custom inverted microscope setup. A supercontinuum pulsed laser (9.2 MHz repetition rate, SuperK NKT Photonics, Birker*d, Denmark) was split into two beams of 488 and 561 nm using a series of filter and mirror combinations. In order to achieve PIE, the beams are directed through separate optical fibers of varying lengths, causing a delay in arrival time between them. This eliminates spectral crosstalk between the detectors. Before entering the microscope, the beams were overlapped by a dichroic beam splitter (LM01-503-25, Semrock) and a customized filter block (zt488/561rpc, zet488/561 m, Chroma Technology). The overlapping beams of light were focused by the objective (×100 TIRF) to a limited diffraction spot on the peripheral membrane of a Cos-7 cell expressing the receptor constructs. In time-tagged time-resolved mode, photons were detected by individual avalanche photodiodes (Micro-Photon Devices). In order to verify the alignment of the system, including the overlap of a confocal volume, a short fluorescently tagged DNA fragment was used. Prior to the experimental samples, positive and negative controls (Figures S2 and S3) were tested to compare the fit parameters.

The excitation beams were focused on the peripheral membranes to measure only membrane-bound receptors. Only the cell's flat, peripheral membrane area was scanned to prevent fluorescence from cytosolic organelles or vesicles. The data collection was performed on one

area of the membrane in each sample. Each area was assessed six times, with each acquisition lasting 10 s. MATLAB scripts were used to calculate each sample's auto- and cross-correlation curves. As described in the previous work, we fit a single component, the 2D diffusion model, to the averaged curves of six consecutive acquisitions per area.

$$G(\tau) = \langle F(t)\, F(t+\tau)\rangle / \langle F(t)\rangle^2 \quad (1)$$

$$G_{GR}(\tau) = \langle F_G(t)\, F_R(t+\tau)\rangle / \langle F_G(t)\rangle\, \langle F_R(t)\rangle \quad (2)$$

The intensity fluctuations were gated using PIE prior to cross-correlation and autocorrelation analyses. The intensity at time $F(t)$ was compared to the intensity at a later time $F\ (t+\tau)$ in an autocorrelation analysis. As a function of time, self-similarity allowed for the interpretation of quantitative information, such as diffusion and particle number. In Equation 1, the intensity fluctuations were divided into 10-s bins and normalized to the square of the average intensity. Cross-correlation uses the intensity fluctuations that occur simultaneously in both channels to infer the interaction of species. The correlation algorithm is represented by Equation 2 and the ratio of the cross-correlation amplitude to the auto-correlation amplitude indicates the proteins in complex, limited by the lower population molecule. The autocorrelation functions were fit to the following model for two-dimensional diffusion in the membrane that accounts for triplet relaxation and dark state dynamics (equation 3).

$$G(\tau) = \left(1 + \frac{T}{1-T} e^{-\tau/\tau T}\right)\left(\frac{1}{\langle N\rangle}\right)\left(\frac{1}{1+\tau/\tau D}\right) + 1 \quad (3)$$

The diffusion coefficient of the sample was calculated using the standard formula given below (Equation 4).

$$D_{\text{eff}} = \frac{\omega^2}{4\tau_D} \quad (4)$$

Finally, the ACF and CCF data were used to calculate the fraction of correlation, f_c (Equation 5).

$$f_c = \frac{\langle N\rangle_{gr}}{\min\left[\left(\langle N\rangle_{gr} + \langle N\rangle_r\right) + \left(\langle N\rangle_{gr} + \langle N\rangle_g\right)\right]} \quad (5)$$

AUTHOR CONTRIBUTIONS

Pradeep Kumar Singh: Conceptualization; methodology; writing – original draft; investigation; data curation; writing – review and editing. **Soyeon Kim:** Conceptualization; methodology; writing – review and editing; investigation. **Adam W. Smith:** Conceptualization; methodology; writing – original draft; funding acquisition; project administration; writing – review and editing.

ACKNOWLEDGMENTS

This work was supported by the National Science Foundation grant CHE-1753060, the Human Frontiers of Science Program No. RGP0059/2019, and the American Lung Association Lung Cancer Discovery Award, LCD-1035035.

CONFLICT OF INTEREST STATEMENT

The authors declare no conflict of interests.

DATA AVAILABILITY STATEMENT

The datasets used during the current study are available from the corresponding author on request.

ORCID

Pradeep Kumar Singh https://orcid.org/0000-0001-8138-244X

Adam W. Smith https://orcid.org/0000-0001-5216-9017

REFERENCES

Appert-Collin A, Hubert P, Crémel G, Bennasroune A. Role of ErbB receptors in cancer cell migration and invasion. Front Pharmacol. 2015;6:283.

Arkhipov A, Shan Y, Das R, Endres Nicholas F, Eastwood Michael P, Wemmer David E, et al. Architecture and membrane interactions of the EGF receptor. Cell. 2013;152(3):557–69.

Bacia K, Kim SA, Schwille P. Fluorescence cross-correlation spectroscopy in living cells. Nat Methods. 2006;3(2):83–9.

Bai X, Sun P, Wang X, Long C, Liao S, Dang S, et al. Structure and dynamics of the EGFR/HER2 heterodimer. Cell Discovery. 2023;9(1):18.

Berger MB, Mendrola JM, Lemmon MA. ErbB3/HER3 does not homodimerize upon neuregulin binding at the cell surface. FEBS Lett. 2004;569(1–3):332–6.

Blumenthal GM, Scher NS, Cortazar P, Chattopadhyay S, Tang S, Song P, et al. First FDA approval of dual anti-HER2 regimen: Pertuzumab in combination with trastuzumab and docetaxel for HER2-positive metastatic breast cancer. Clin Cancer Res. 2013;19(18):4911–6.

Brown BP, Zhang Y-K, Kim S, Finneran P, Yan Y, Du Z, et al. Allele-specific activation, enzyme kinetics, and inhibitor sensitivities of EGFR exon 19 deletion mutations in lung cancer. Proc Natl Acad Sci. 2022;119(30):e2206588119.

Carpenter G. ErbB4: mechanism of action and biology. Exp Cell Res. 2003;284:66–77.

Carraway KL, Sweeney C. Localization and modulation of ErbB receptor tyrosine kinases. Curr Opin Cell Biol. 2001;13(2):125–30.

Catapano C, Rahm JV, Omer M, Teodori L, Kjems J, Dietz MS, et al. Biased activation of the receptor tyrosine kinase HER2. Cell Mol Life Sci. 2023;80(6):158.

Christie S, Shi X, Smith AW. Resolving membrane protein-protein interactions in live cells with pulsed interleaved excitation fluorescence cross-correlation spectroscopy. Acc Chem Res. 2020; 53(4):792–9.

Citri A, Skaria KB, Yarden Y. The deaf and the dumb: the biology of ErbB-2 and ErbB-3. Exp Cell Res. 2003;284(1):54–65.

Citri A, Yarden Y. EGF–ErbB signalling: towards the systems level. Nat Rev Mol Cell Biol. 2006;7(7):505–16.

Clayton AHA, Walker F, Orchard SG, Henderson C, Fuchs D, Rothacker J, et al. Ligand-induced dimer-tetramer transition during the activation of the cell surface epidermal growth factor receptor-a multidimensional microscopy analysis. J Biol Chem. 2005;280(34):30392–9.

Dawson JP, Bu Z, Lemmon MA. Ligand-induced structural transitions in ErbB receptor extracellular domains. Structure. 2007; 15(8):942–54.

Diwanji D, Trenker R, Thaker TM, Wang F, Agard DA, Verba KA, et al. Structures of the HER2–HER3–NRG1β complex reveal a dynamic dimer interface. Nature. 2021;600(7888):339–43.

Du Z, Brown BP, Kim S, Ferguson D, Pavlick DC, Jayakumaran G, et al. Structure–function analysis of oncogenic EGFR kinase domain duplication reveals insights into activation and a potential approach for therapeutic targeting. Nat Commun. 2021; 12(1):1382.

El-Gamal MI, Mewafi NH, Abdelmotteleb NE, Emara MA, Tarazi H, Sbenati RM, et al. A review of HER4 (ErbB4) kinase, its impact on cancer, and its inhibitors. Molecules. 2021;26:7376.

Endres NF, Barros T, Cantor AJ, Kuriyan J. Emerging concepts in the regulation of the EGF receptor and other receptor tyrosine kinases. Trends Biochem Sci. 2014;39(10):437–46.

Endres Nicholas F, Das R, Smith Adam W, Arkhipov A, Kovacs E, Huang Y, et al. Conformational coupling across the plasma membrane in activation of the EGF receptor. Cell. 2013;152(3): 543–56.

Freed DM, Bessman NJ, Kiyatkin A, Salazar-Cavazos E, Byrne PO, Moore JO, et al. EGFR ligands differentially stabilize receptor dimers to specify signaling kinetics. Cell. 2017;171:683–695.e18.

Fujiwara S, Yamamoto-Ibusuki M, Yamamoto Y, Yamamoto S, Tomiguchi M, Takeshita T, et al. The localization of HER4 intracellular domain and expression of its alternately-spliced isoforms have prognostic significance in ER+ HER2-breast cancer. Oncotarget. 2014;5:3919–30.

Garrett TPJ, McKern NM, Lou M, Elleman TC, Adams TE, Lovrecz GO, et al. The crystal structure of a truncated ErbB2 ectodomain reveals an active onformation, poised to interact with other ErbB receptors. Mol Cell. 2003;11:495–505.

Graus-Porta D, Beerli RR, Daly JM, Hynes NE, Miescher F. ErbB-2, the preferred heterodimerization partner of all ErbB receptors, is a mediator of lateral signaling. EMBO J. 1997;16:1647–55.

Haryuni RD, Watabe S, Yamaguchi A, Fukushi Y, Tanaka T, Kawasaki Y, et al. Negative feedback regulation of ErbB4 tyrosine kinase activity by ERK-mediated non-canonical phosphorylation. Biochem Biophys Res Commun. 2019;514(2):456–61.

Huang Y, Bharill S, Karandur D, Peterson SM, Marita M, Shi X, et al. Molecular basis for multimerization in the activation of the epidermal growth factor receptor. Elife. 2016;5:e14107.

Hynes NE, MacDonald G. ErbB receptors and signaling pathways in cancer. Curr Opin Cell Biol. 2009;21:177–84.

Jaulin-Bastard F, Saito H, Le Bivic A, Ollendorff V, Marchetto S, Birnbaum D, et al. The ErbB2/HER2 receptor differentially interacts with ERBIN and PICK1 PSD-95/DLG/ZO-1 domain proteins. J Biol Chem. 2001;276(18):15256–63.

Jeong J, Kim W, Kim LK, VanHouten J, Wysolmerski JJ. HER2 signaling regulates HER2 localization and membrane retention. PLoS One. 2017;12(4):e0174849.

Kaliszewski MJ, Shi X, Hou Y, Lingerak R, Kim S, Mallory P, et al. Quantifying membrane protein oligomerization with fluorescence cross-correlation spectroscopy. Methods. 2018;140-141: 40–51.

Karl K, Paul MD, Pasquale EB, Hristova K. Ligand bias in receptor tyrosine kinase signaling. J Biol Chem. 2020;295:18494–507.

Kiavue N, Cabel L, Melaabi S, Bataillon G, Callens C, Lerebours F, et al. ErbB3 mutations in cancer: biological aspects, prevalence and therapeutics. Oncogene. 2020;39:487–502.

Kim JY, Jung HH, Do IG, Bae SY, Lee SK, Kim SW, et al. Prognostic value of ErbB4 expression in patients with triple negative breast cancer. BMC Cancer. 2016;16:138.

Kol A, Terwisscha Van Scheltinga AGT, Timmer-Bosscha H, Lamberts LE, Bensch F, De Vries EGE, et al. HER3, serious partner in crime: therapeutic approaches and potential biomarkers for effect of HER3-targeting. Pharmacol Ther. 2014; 143(1):1–11.

Kumagai S, Koyama S, Nishikawa H. Antitumour immunity regulated by aberrant ERBB family signalling. Nat Rev Cancer. 2021;21:181–97.

Lemmon MA, Schlessinger J. Cell signaling by receptor tyrosine kinases. Cell. 2010;141(7):1117–34.

Lemmon MA, Schlessinger J, Ferguson KM. The EGFR family: not so prototypical receptor tyrosine kinases. Cold Spring Harb Perspect Biol. 2014;6(4):a020768.

Lucas LM, Dwivedi V, Senfeld JI, Cullum RL, Mill CP, Piazza JT, et al. The yin and Yang of ERBB4: tumor suppressor and oncoprotein. Pharmacol Rev. 2022;74(1):18–47.

Martin-Fernandez ML. A perspective of fluorescence microscopy for cellular structural biology with EGFR as witness. J Microsc. 2023;291(1):73–91.

Müller BK, Zaychikov E, Bräuchle C, Lamb DC. Pulsed interleaved excitation. Biophys J. 2005;89(5):3508–22.

Muraoka-Cook RS, Feng SM, Strunk KE, Earp SH. ErbB4/HER4: role in mammary gland development, differentiation and growth inhibition. J Mammary Gland Biol Neoplasia. 2008; 13(2):235–46.

Nagy P, Claus J, Jovin TM, Arndt-Jovin DJ. Distribution of resting and ligand-bound ErbB1 and ErbB2 receptor tyrosine kinases in living cells using number and brightness analysis. Proc Natl Acad Sci. 2010;107(38):16524–9.

Ogiso H, Ishitani R, Nureki O, Fukai S, Yamanaka M, Kim J-H, et al. Crystal structure of the complex of human epidermal growth factor and receptor extracellular domains. Cell. 2002; 110:775–87.

Okada T, Miyagi H, Sako Y, Hiroshima M, Mochizuki A. Origin of diverse phosphorylation patterns in the ERBB system. Biophys J. 2022;121(3):470–80.

Phillips GDL, Fields CT, Li G, Dowbenko D, Schaefer G, Miller K, et al. Dual targeting of HER2-positive cancer with trastuzumab emtansine and pertuzumab: critical role for neuregulin

blockade in antitumor response to combination therapy. Clin Cancer Res. 2014;20(2):456–68.
Plowman GD, Culouscou J-M, Whitney GS, Green JM, Carlton GW, Foy L, et al. Ligand-specific activation of HER4/-pl80erbB4, a fourth member of the epidermal growth factor receptor family (receptor tyrosine kne/ERBB4 gene product). Proc Natl Acad Sci. 1993;90:1746–50.
Pryor MMC, Steinkamp MP, Halasz AM, Chen Y, Yang S, Smith MS, et al. Orchestration of ErbB3 signaling through heterointeractions and homointeractions. Mol Biol Cell. 2015; 26(22):4109–23.
Qiu C, Tarrant MK, Choi SH, Sathyamurthy A, Bose R, Banjade S, et al. Mechanism of activation and inhibition of the HER4/ErbB4 kinase. Structure. 2008;16(3):460–7.
Riese DJ, Kim ED, Elenius K, Buckley S, Klagsbrun M, Plowman GD, et al. The epidermal growth factor receptor couples transforming growth factor-α, heparin-binding epidermal growth factor-like factor, and amphiregulin to neu, ErbB-3, and ErbB-4*. J Biol Chem. 1996;271(33):20047–52.
Roskoski R. ErbB/HER protein-tyrosine kinases: structures and small molecule inhibitors. Pharmacol Res. 2014;87:42–59.
Sankaran J, Wohland T. Current capabilities and future perspectives of FCS: super-resolution microscopy, machine learning, and in vivo applications. Commun Biol. 2023;6(1):699.
Segers VFM, Dugaucquier L, Feyen E, Shakeri H, De Keulenaer GW. The role of ErbB4 in cancer. Cell Oncol. 2020; 43:335–52.
Sierke SL, Cheng K, Kim H-H, Koland JG. Biochemical characterization of the protein tyrosine kinase homology domain of the ErbB3 (HER3) receptor protein. Biochem J. 1997;322: 757–63.
Steinkamp MP, Low-Nam ST, Yang S, Lidke KA, Lidke DS, Wilson BS. ErbB3 is an active tyrosine kinase capable of homo- and Heterointeractions. Mol Cell Biol. 2014;34(6):965–77.
Stoneman MR, Raicu V. Fluorescence-based detection of proteins and their interactions in live cells. J Phys Chem B. 2023; 127(21):4708–21.
Sweeney C, Lai C, Riese DJ, Diamonti AJ, Cantley LC, Carraway KL. Ligand discrimination in signaling through an ErbB4 receptor homodimer. J Biol Chem. 2000;275(26):19803–7.
Tao RH, Maruyama IN. All EGF(ErbB) receptors have preformed homo- and heterodimeric structures in living cells. J Cell Sci. 2008;121(19):3207–17.
Tebbutt N, Pedersen MW, Johns TG. Targeting the ERBB family in cancer: couples therapy. Nat Rev Cancer. 2013;13:663–73.
Tidcombe H, Jackson-Fisher A, Mathers K, Stern DF, Gassmann M, Golding JP. Neural and mammary gland defects in ErbB4 knockout mice genetically rescued from embryonic lethality. Proc Natl Acad Sci. 2003;100(14):8281–6.
Trenker R, Diwanji D, Bingham T, Verba KA, Jura N. Structural dynamics of the active HER4 and HER2/HER4 complexes is finely tuned by different growth factors and glycosylation. Elife. 2023;12:RP92873.
Van Lengerich B, Agnew C, Puchner EM, Huang B, Jura N. EGF and NRG induce phosphorylation of HER3/ERBB3 by EGFR using distinct oligomeric mechanisms. Proc Natl Acad Sci U S A. 2017;114(14):E2836–45.
Váradi T, Schneider M, Sevcsik E, Kiesenhofer D, Baumgart F, Batta G, et al. Homo- and Heteroassociations drive activation of ErbB3. Biophys J. 2019;117(10):1935–47.
Walker RA. The ErbB/HER type 1 tyrosine kinase receptor family. J Pathol. 1998;185(3):234–5.
Weitsman G, Barber PR, Nguyen LK, Lawler K, Patel G, Woodman N, et al. HER2-HER3 dimer quantification by FLIM-FRET predicts breast cancer metastatic relapse independently of HER2 IHC status. Oncotarget. 2016;7(32):51012–26.
Xu J, Gong L, Qian Z, Song G, Liu J. ErbB4 promotes the proliferation of gastric cancer cells via the PI3K/Akt signaling pathway. Oncol Rep. 2018;39(6):2892–8.
Yarden Y, Sliwkowski MX. Untangling the ErbB signalling network. Nat Rev Mol Cell Biol. 2001;2(2):127–37.

SUPPORTING INFORMATION

Additional supporting information can be found online in the Supporting Information section at the end of this article.

How to cite this article: Singh PK, Kim S, Smith AW. HER4 is a high-affinity dimerization partner for all EGFR/HER/ErbB family proteins. Protein Science. 2024;33(10):e5171. https://doi.org/10.1002/pro.5171